Integrated Simulations of H-mode Operation in ITER including Core Fuelling, Divertor Detachment and ELM Control

A.R. Polevoi[1], A. Loarte[1], R. Dux[2], T. Eich[2], E. Fable[2],
S. Maruyama[1], S.Yu. Medvedev[3], F. Köchl[4], V.E. Zhogolev[5]

[1]*ITER Organization, Route de Vinon-sur-Verdon, 13067 St Paul Lez Durance, France*
[2]*Max-Planck Inst. für Plasmaphysik, Boltzmanstraße 2, D-85748 Garching, Germany*
[3] *Keldysh Institute of Applied Mathematics, Miusskaya 4, 125047 Moscow, Russia*
[4]*Atominstitut, Technische Universität Wien, Stadionallee 2, 1020 Vienna, Austria*
[5]*NRC "Kurchatov Institute", Kurchatov sq. 1, 123098 Moscow, Russia*

E-mail: Alexei.Polevoi@iter.org

Abstract. ELM mitigation for divertor protection is one of the main factors affecting plasma fuelling and detachment control at full current operation. Here we derive the scaling for the operational space, where the ELM mitigation for divertor protection is not required and parameters of ELM-pacing pellet injection are determined by the tungsten control. The applied experimental scaling eliminates the uncertainty connected with the ELM affected area and enables the definition of the operating space through global plasma parameters. Our evaluation is based on this empirical scaling for ELM power load, and on the scaling for the pedestal height limit based on the stability code predictions. In particular, the analysis revealed that for the pedestal height predicted by EPED1+SOLPS scaling the ELM mitigation for divertor protection is not required in half-field operation, but with conservative assumptions on the power flux ELM mitigation is required for rather low currents, I_p > 5 MA. The pellet and gas fuelling requirements compatible with control of plasma detachment, tungsten accumulation and the H-mode operation are assessed by 1.5D transport simulations for full tungsten re-deposition and with the most conservative assumption of zero prompt re-deposition. The tungsten influx as a function of the ELM frequency is derived on the basis of consistent core-divertor simulations.

1. Introduction

Integrated simulations of ITER H-mode plasmas including gas and pellet fuelling for core and edge density/divertor power load control and pellet pacing for ELM control have been carried out and it was shown that the flexibility of the ITER fuelling systems enables high Q ITER operation [1]. These simulations have shown that ELM control to ensure appropriate divertor target erosion lifetime is one of the main factors affecting plasma fuelling and detachment control at full current operation in ITER. At lower plasma currents, the power fluxes during ELMs at the ITER divertor are not expected to cause large scale erosion [2]. For these lower current levels the requirements for the control of ELMs, such as through frequency control by pellet pacing, are determined by the control of the tungsten concentration in the core plasma required to keep plasma in the H-mode regime [2, 3]. In the present work we extend the analysis in [2, 3] by performing integrated simulations of ITER plasmas including the core and edge fuelling requirements to ensure appropriate fusion performance and control of divertor power loads together with requirements for ELM control by pellet pacing to achieve an acceptable divertor erosion and core W level. To determine the ELM control requirements for acceptable divertor erosion, we have evaluated first the H-mode operational space for which ELM control is not required to achieve acceptable divertor erosion lifetime in ITER. This has been done by applying the empirical scaling for the ELM power flux in [4], where the peak ELM energy density at the divertor (ε) is found to be proportional to the pedestal plasma pressure with $\varepsilon \sim K\, p_{ped}$, where K = 1-4.5 covers the range of experimental data, and the expected pedestal plasma parameters in ITER are evaluated from MHD stability predictions [5]. This approach is based on global plasma parameters and provides a refined evaluation with respect to the approach in [2], which considered the area over which ELMs deposit their energy at the divertor as a variable

parameter. The estimate of the H-mode operational space with acceptable ELMs is described in section 2.

As it is discussed in [2], in the range of plasma parameters where the ELMs are acceptable from the point of view of the erosion of the divertor, the limitations on the ELM size and frequency are determined by the requirements of the control of plasma contamination by tungsten caused by ELMs. In section 3 we derived the scalings for tungsten influx to the plasma core as a function of the ELM size basing on combined simulations by ASTRA, STRAHL, and SOLPS codes described in [3]. Using these scalings we estimate the tungsten influx from the ELMs for the ITER H-mode operation, by applying the continuous ELM and pellet models [1].

Including the time-varying W source during an ELM and the mechanisms for W outflux and influx during them is, however, expected to lead to stringent limits on ELM energy losses on the basis of previous studies [3]. Therefore, simulations including the effect of the time-varying W influx during the ELM as well as the effects of pellet pacing on the fuelling efficiency of high field side pellets are performed to refine the above estimates with more realistic modelling assumptions and updated design of the ITER fuelling system. In section 4, we describe the impact of the discrete pellet and ELM models on the pellet injection requirements.

In our consideration we use the following units, seconds for time, t, Δt, MW for power P, MJ for energies W, ΔW, m, m^2 and m^3 for size a, R, area S and volume V, MA for current I_p, T for magnetic field B, $10^{19} m^{-3}$ for density n, keV for temperatures T, kPa for pressure p, and Hz for frequency f. Thus, using the listed variables we omit, when possible, the units in the formulas below.

2. Operation space with tolerable ELMs

The maximum power density in ELMs in ITER is limited by melting of the divertor monoblock surface, ε_{max}:

$$\varepsilon_{\|} \sin(\alpha) \, (t_{ELM}/t_{ELM,0})^{-0.5} \leq \varepsilon_{max}, \qquad (1)$$

where ε_{max} is the melting limit in MJm^{-2}, $\varepsilon_{\|}$ is the maximum power density during ELM along the field line, α is the angle of inclination of the magnetic field line to the monoblock surface, $t_{ELM}/t_{ELM,0}$ is the normalised time of the exposition of the ELM power on the divertor surface.

Our analysis of the operational space with ELMs tolerable to divertor erosion is based on the following assumptions: we assume that for 15 MA we will have an ELM rise time of 250 microseconds, fall-down time of 500 μs [6] and a power flux in the region of 5-10 MWm^{-2} between ELMs. For these conditions the W melting threshold for a 5-10 mm thick W monoblock is $\varepsilon_{max} \approx 0.6$ MJm^{-2}. This corresponds to a parallel energy density of 12.2 MJm^{-2} for the inner divertor with $\alpha_{in} = 3.7^o(3/q_{95}) + 1^o \approx 0.0228\ (1+0.77\ B/I_p)\ I_p/B$ [rad], where $3.7^o(3/q_{95})$ is the field line incidence angle, 1^o is the toroidal inclination of the target , $q_{95} = 8.49\ B/I_p$ is the edge safety factor, and 13.7 MJm^{-2} for the outer divertor with $\alpha_{out} = 3.2^o(3/q_{95}) + 1^o \approx 0.0197\ (1+0.88\ B/I_p)\ I_p/B$ [rad]. Above these values the W monoblock surface would melt. For lower current operation the allowed value of 0.6 MJm^{-2} is increased proportionally to $(t_{ELM})^{0.5}$, as the surface temperature rise during the ELM scales with $Energy/(time)^{0.5}$, to take into account the longer timescale of the ELM energy flux due to both the lower pedestal temperature and longer SOL connection length assuming that t_{ELM} is correlated with the ion sound speed. Then the normalised ELM timescale is $t_{ELM}/t_{ELM,0} = (q_{95}/3)\ (T_{ref}/T_{ped})^{0.5}$, where T_{ped} is the temperature at the pedestal top, $T_{ref} = 4.2$ keV is the pedestal temperature for the reference case for baseline 15 MA ITER scenario with the pedestal density $n_{ped}/n_G = g = 0.70$, with $n_G = 10\ I_p/\pi a^2$.

According to the scaling, based on the ASDEX-U and JET experiments, the maximum ELM energy density to the divertor parallel to the magnetic field line is proportional to the pressure at the pedestal top [4]:

$$\varepsilon_{\parallel} = 0.084\ K\ n_{ped}T_{ped}q_{.95} = 0.713\ K\ n_{ped}T_{ped}B/I_p, \qquad (2)$$

where K = 1-4.5. The range of K = 1-4.5 extends from the most optimistic assumptions to the most pessimistic assumptions. The optimistic value K=1 corresponds to a symmetric ELM energy flux distribution between the inner and outer divertors, $\varepsilon_{\parallel,in} = \varepsilon_{\parallel,out}$. This corresponds to $\varepsilon_{\parallel}$ = 9.5 MJm^{-2} for the baseline ITER case with B/I_p = 15 MA/5.3T, n_{ped} = 8 10^{19} m^{-3}, $T_{i,ped}+T_{e,ped}$= 9.4 keV, and to $\varepsilon_{\parallel}$ =2.4 MJm^{-2} for B/I_p = 7.5 MA/2.65T case. The value K=4.5 corresponds to $\varepsilon_{\parallel,out}$ = 3 $\varepsilon_{\parallel,out}$(K=1) = 28.5 MJm^{-2} for 15 MA/5.3T and 7.2 MJm^{-2} for 7.5 MA/2.65T, and to $\varepsilon_{\parallel,in}$ = 1.5 $\varepsilon_{\parallel,out}$ = 4.5 $\varepsilon_{\parallel,out}$(K=1). The factor 3 comes from the uncertainty due to the experimental data scattering and the factor of 1.5 comes from the fact that although the total ELM energy at the inner divertor is larger than at the outer one by about a factor of 2, the footprint mapped to the outer midplane is broader by about a factor of 2. This then just leaves the difference in parallel area at the inner and outer divertors which is proportional to the inverse ratio of the toroidal fields at the strike points at both divertors and this is about B_{in}/B_{out} = 1.3 in ITER; to be conservative we take B_{in}/B_{out} = 1.5.

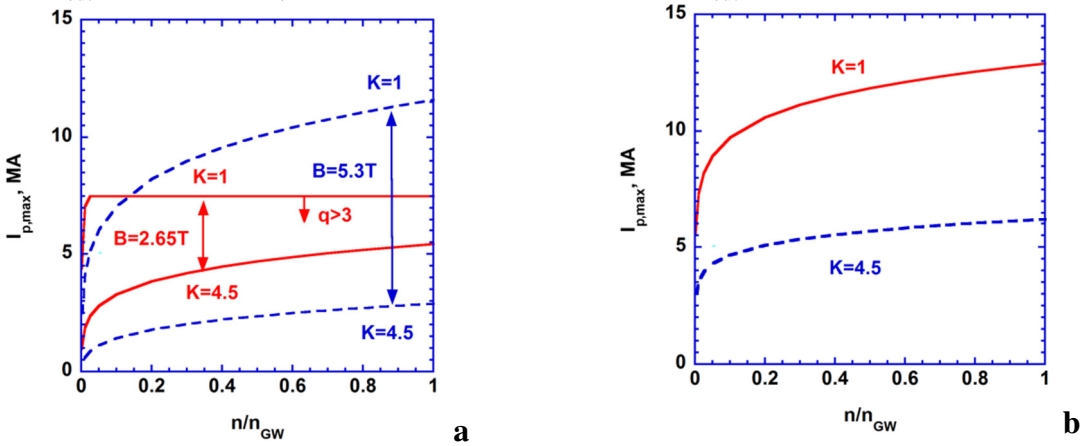

Figure 1. Maximum plasma current predicted by the optimistic and conservative assumptions for the acceptable uncontrolled ELM power loads: density scan with B=const (a); with q_{95}=3 (b).

Taking into account the assumptions above, we can derive the upper and lower estimates for the ELM load from the equation (2): 0.713 K $\sin(\alpha_{in})(t_{ELM}/t_{ELM,0})^{-0.5} n_{ped}T_{ped}B/I_p$ = 0.6.

Note that according to the EPED1+SOLPS predictions [1] the pedestal pressure in ITER can be expressed as:

$$p_{ped} = 3.2\ n_{ped}\ T_{e,ped} = 2.17\ B^{0.84}I_p. \qquad (3)$$

This relation gives us the expressions for the pedestal temperature, T_{ped} = 0.85 $B^{0.84}g^{-1}$, and for the normalized ELM timescale, $(t_{ELM}/t_{ELM,0})^{0.5}$ = 2.48 $B^{0.29}g^{0.25}/I_p^{0.5}$, $\varepsilon_{\parallel}$= 0.486 K $B^{1.84}$. Finally assuming $\sin(\alpha_{in}) \approx 0.0228\ (1+0.77\ B/I_p)\ I_p/B$, we get the equations for the upper boundary for plasma current for the most optimistic and the most conservative case for which uncontrolled ELMs would be acceptable from the divertor erosion point of view :

$$I_{p,opt} = 26.2\ g^{0.17}\ B^{-0.37}/(1+0.77B/I_{p,opt})^{2/3}, \qquad (4.1)$$
$$I_{p,con} = 9.62\ g^{0.17}\ B^{-0.37}/(1+0.77B/I_{p,con})^{2/3}. \qquad (4.2)$$

These boundaries calculated from equations (4) are shown in figure 1 both for density scans with fixed magnetic fields (figure 1a), and with fixed safety factor (figure 1b). With the optimistic assumptions (K=1) ELM control for divertor protection is not required for half-field in the whole density range up to 7.5 MA, for full-field the maximum current is limited by 10-11.5 MA for 0.5 < g <1. With pessimistic assumptions (K=4.5) for 0.5 < g <1 such operating is limited by 4.5-5.5 MA for B=2.65 T, and ~ 2.5 – 3 MA for B=5.3 due to the higher pedestal pressure and the lower area for parallel flow associated with high field operation. In the following section we estimate the requirements to ELM pacing from the point of view of the control of tungsten accumulation compatible with the H-mode operation.

3. Estimate of tungsten accumulation

From experimental observations it is known [7] that the ELM size and frequency are correlated with the SOL power flow as

$$\Delta W_{ELM}\, f_{ELM} = \alpha\, P_{sol}, \qquad (5)$$

where we take α = 0.2 -0.4 covering small ELMs, $\Delta W_{ELM}/W_{ped} << 1$ to large ELMs. From the scaling (3) it is possible to estimate the pedestal energy, $W_{ped} = 3\, p_{ped}\, V = 2.68\, B^{0.84} I_p$, for the ITER plasma with volume V=820 m^3. For 15MA/2.65T W_{ped} = 163 MJ, while for 7.5MA/2.65T W_{ped} = 45.5 MJ. Size of the natural ELMs can be estimated from the empirical relation [8], $\Delta W_{ELM}/W_{ped} = 0.064/(\nu_p^*)^{1/3} \approx 0.118\, B^{0.224}/g$ ~ 0.15-0.2, where $\nu_p^* = 8.69\ 10^{-4}\, \pi R q_{95}\, n_{ped}/T_{ped}^2 \approx 0.16\, g^3 B^{-0.68}$ is the normalised pedestal collisionality. Then, $\Delta W_{ELM} \approx 0.315\, I_p B^{1.064}/g$. Note that the natural ELMs in ITER are pretty large, thus we have to assume α ~ 0.2 – 0.4 and treat them as conductive type ELMs. For half-field q=3 case we obtain $\Delta W_{ELM} \approx 6.7/g$, f_{ELM} ~ 0.03 - 0.06 g P_{sol}. For full-field q=3 operation we obtain $\Delta W_{ELM} \approx 28/g$, f_{ELM} ~ 0.007-0.014 g P_{sol}.

In order to determine the ELM frequency required for control of the core W concentration, we have used the results of previous simulations of W divertor production and transport [3] and evaluated the time-averaged W influx into the confined plasma for a range of controlled ELM frequencies, edge power flows, P_{sol}, and assumptions regarding W re-deposition during the ELM. We also analyse the impact of discrete influx pulses of tungsten sputtered by ELMs that reach the plasma core on the H-mode operation.

To estimate the dynamics of tungsten accumulation we derived the scalings for tungsten influx to the plasma core as a function of the ELM size based on combined simulations of ITER scenarios by ASTRA, STRAHL, and SOLPS codes described in [3]. It was found [3] that delay time after the ELM, $\Delta t_{d,W}$, and duration of the pulse of tungsten sputtered by ELM, which reaches the plasma core, $\Delta t_{p,W}$, depend on the ELM size, and could be approximated as:

$$\Delta t_{d,W} = 0.3 + 1.8 \exp(-3.7\Delta W_{ELM}),\ \Delta t_{p,W} = 1.3 + 7 \exp(-2.2\, \Delta W_{ELM})\ [\text{ms}]. \qquad (6)$$

For the worst case without prompt re-deposition of the sputtered tungsten the number of particles entering the core plasma after the ELM can be approximated as: $\Delta N_W = 2.8\ 10^{18}(1 - \exp(-\Delta W_{ELM}^{1.6}))$, which together with eq. (5) will give the expression for prompt and time averaged tungsten influxes:

$$S_W = \Delta N_W/\Delta t_{p,W} = 2.8\ 10^{21}(1 - \exp(-\Delta W_{ELM}^{1.6}))/(1.3 + 7 \exp(-2.2\Delta W_{ELM})), \qquad (7.1)$$

$$\langle S_W \rangle = \Delta N_W\, f_{ELM} = 2.8\ 10^{18}\, \alpha\, P_{sol}\, (1 - \exp(-\Delta W_{ELM}^{1.6}))/\Delta W_{ELM}. \qquad (7.2)$$

The prompt and averaged tungsten influxes are shown in figure 2. The solid lines correspond to P_{sol} = 50 MW with small ELMs (α=0.2). The dashed lines correspond to P_{sol} = 100 MW with small ELMs (α=0.2) or to P_{sol} = 50 MW with large ELMs (α=0.4). Note that the average influx has a maximum at frequencies f ~ 30 Hz required for ELM pacing with ΔW_{ELM} = 0.6 MJ [1]. Meanwhile the prompt flux noticeably drops $S_W(30Hz)/S_{W,max}$ ~ 0.25. Thus, the impact of the prompt ELM/pellet modelling could lead to different results from those obtained with the continuous ELM/pellet model [1]. This difference is discussed in the section 4.

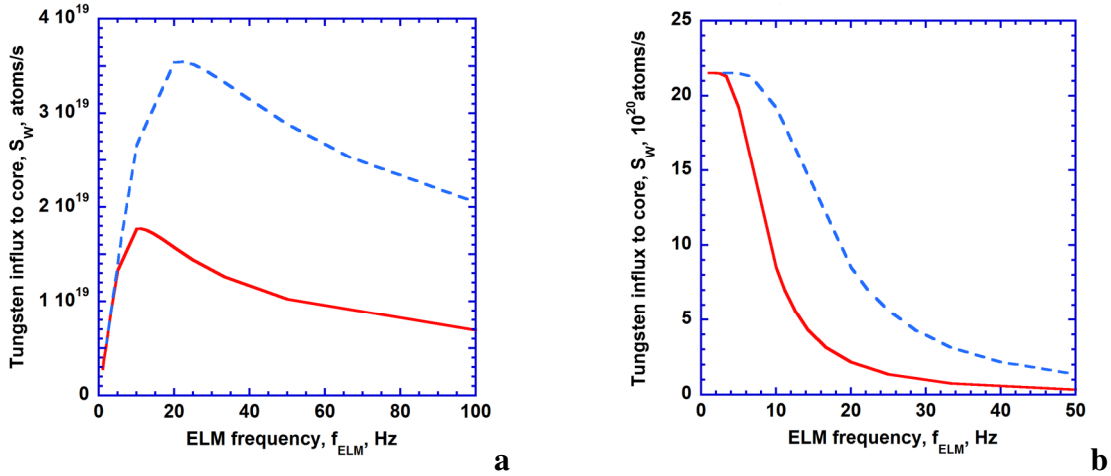

Figure 2. Influx of tungsten sputtered by ELMs to the core without prompt W-re-deposition for P_{sol}=100 MW (dashed line) and P_{sol}=50 MW (solid line): a – time averaged flux (see equation 7.1); b- prompt influx (see equation 7.2).

4. Impact of the discrete ELM modelling on plasma performance

In our simulations we apply 1.5D transport simulations of core plasma with boundary conditions and edge fuelling consistent with the SOLPS simulations [10] with transport coefficients in the pedestal chosen to provide the inter-ELM pedestal height consistent with the EPED1+SOLPS predictions [5], neon injection and gas puffing for the control of the power loads, high field side pellet injection for core plasma fuelling, low field side pellet injection for ELM control and we consider both cases with and without tungsten prompt re-deposition.

For modelling of the heat and transport we use the scaling-based model used earlier with the continuous ELM/pellet treatment for consistent description of the integrated fuelling, ELM and divertor control analysis [1]. Boundary conditions and inter-ELM pedestal parameters were calculated consistently with EPED1 and SOLPS predictions [1] based on the scalings in [10]. Core modelling was performed by 1.5D transport analysis on the basis of the Automated System for Transport Analysis (ASTRA) [11] with the ZIMPUR code for impurities transport [12] using the results of ASTRA-STRAHL and SOLPS simulations [3] for tungsten influxes (equations 6, 7). For the simulation of impurity ions we assume boundary conditions which provide the quasi-neutrality, $G_i = n_i G_e/\sum Z_i n_i$, where n_i, Z_i, G_i are the ion density, charge state and out-flux, G_e is the outflux of the electrons.

In our present studies we extend the considerations in [1] by modelling of discrete ELMs [3] and of discrete pellets [9]. For prompt ELMs we consider diffusive and convective ELM models [3] for the particle losses with ELMs. The diffusive ELM is modelled by increased particle diffusivity, resulting in a flattening of fuel and impurity profiles in the ELM–affected area, Δ_{ELM}, while the convective ELM ejects particles as a net outward convective velocity over the same area. The ELM frequency, f_{ELM}, is considered as a variable parameter

controlled by HFS-fuelling and LFS-pacing pellets, $f_{pel}=f_{ELM}= f_{HFS} + f_{LFS}$. Note that post pellet reversed density gradients create additional out-pumping of tungsten in the ELM-affected area due to neoclassical transport effects. To simulate the ELMs the appropriate transport coefficients were increased for Δt_{ELM} ~1 ms to provide the energy loss, ΔW_{ELM}, calculated from the experimental scaling (equation 5). For tungsten inter-ELM transport we assume neoclassical coefficients. During the ELM we assume for W in the ELM affected area the same transport assumptions which are used to simulate the ELM loss for the main ions.

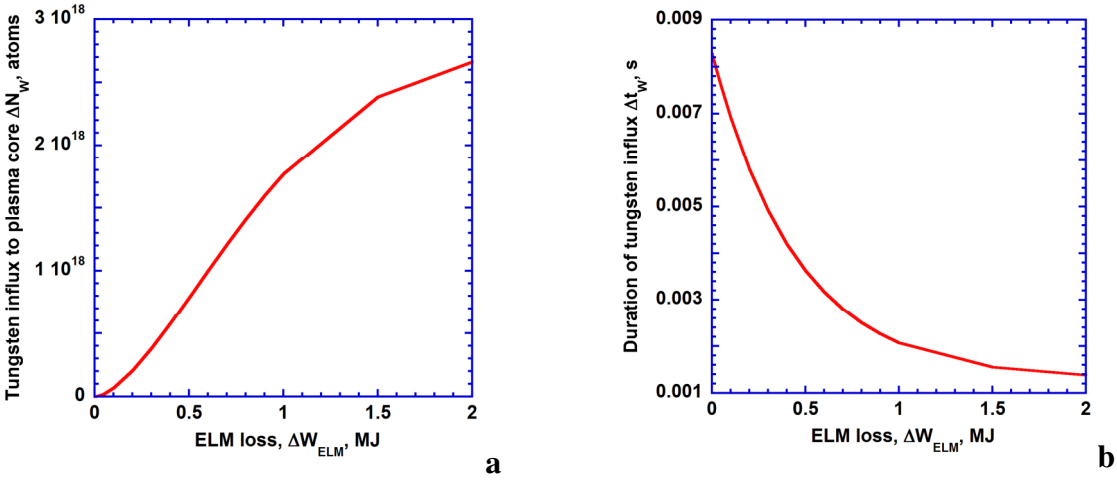

Figure 3. Characteristics of the post-ELM tungsten influx pulse which reaches plasma w/o prompt re-deposition: a- pulse size; b- pulse duration.

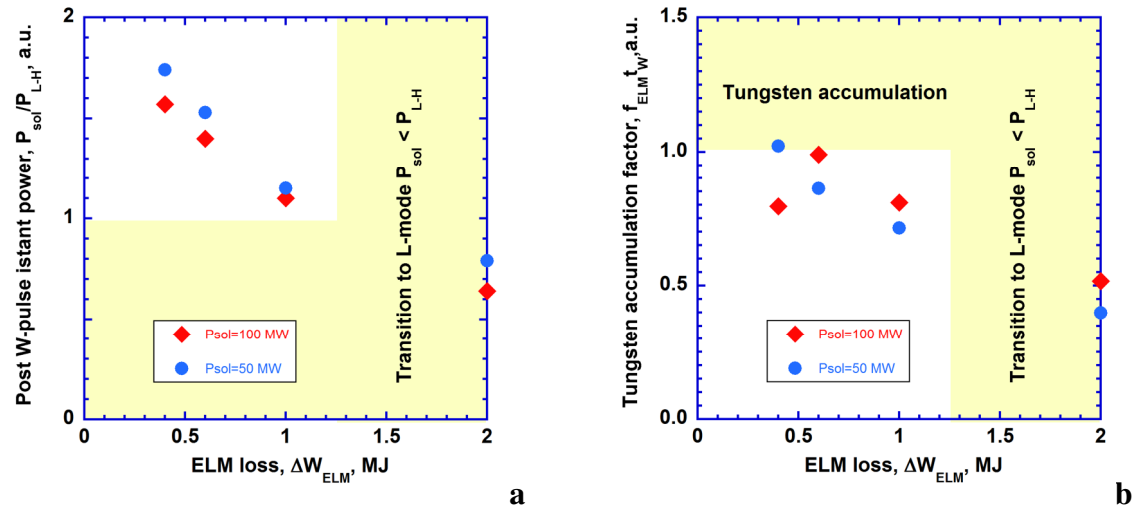

Figure 4. H-mode operating space for B/I_p = 5.3 T/15 MA with pre-ELM power to SOL P_{sol}=100 MW, and for B/I_p = 2.65 T/7.5 MA with pre-ELM P_{sol}=50 MW w/o prompt tungsten re-deposition for small ELMs, $f_{ELM}=0.2P_{sol}/\Delta W_{ELM}$: a- post W-pulse power to SOL over the L-H threshold, P_{sol}/P_{L-H}, [13]; b- tungsten accumulation factor, $F_{W,a}= f_{ELM}t_W$.

With the discrete ELM modelling we address two key issues: the peak W radiation at each ELM, which could cause H- to L-mode transitions as observed in some experiments; and the core W accumulation on long time scales. The characteristics of the ELM-caused tungsten pulses, which reach the plasma core, are displayed in figure 3 for the case without prompt tungsten re-deposition. It is clear that W-pulse size and duration saturate at ΔW_{ELM}~ 2 MJ. Thus, to address the instant effects of a single ELM it is sufficient to consider ELM of such size. When the W-pulse is large enough, it can increase strongly plasma radiation, which promptly reduces the power to the SOL, P_{sol}, below the L-H threshold [13], P_{LH}: $P_{sol}/P_{LH} < 1$, leading to an H to L transition possibly followed by a disruption.

To characterize the effect of tungsten accumulation it is useful to introduce the tungsten accumulation factor, $F_{W,a}= f_{ELM} \times t_W$, where the full tungsten cycle time, t_W, includes the post-ELM W-pulse delay and duration times, $\Delta t_{d,W}$, $\Delta t_{p,W}$ (see equation 6), as well as the recovery time, $t_{W,rec}$, i.e. time required to remove the tungsten, delivered by a W-pulse, from the plasma core: $t_W = \Delta t_{d,W} + \Delta t_{p,W} + t_{W,rec}$. The recovery time, $t_{W,rec}$ is calculated on the basis of time-dependent 1.5D transport modelling. Note that the accumulation factor greater than one, $F_{W,a} \geq 1$ means that tungsten delivered by W-pulse cannot be fully removed between ELMs, which causes tungsten accumulation, gradual increase of core radiation, reduction of the power flux to the SOL, $P_{sol}/P_{LH} \rightarrow 1$ and a follow-up transition to L-mode. The results of simulations of post-W-pulse plasma parameters are presented in figure 4. According to these simulations, the pulses of tungsten which reach the core w/o prompt re-deposition, produced by ELMs with rather moderate size, $\Delta W_{ELM} \geq$ 1.1-1.2 MJ, can increase prompt radiation to the level sufficient to trigger the H-L transition, $P_{sol}/P_{LH} < 1$ (figure 4a). For small ELMs (α=0.2) assumed in our modelling the whole range of pellet pacing frequencies foreseen in ITER, $f_{pel} \leq 32$ Hz does not cause the tungsten accumulation.

When sizeable W prompt re-deposition is considered, there are no issues regarding both the transient increase of plasma radiation following the ELM as well as of long timescale W accumulation because the W influxes from the divertor are found to be very typically ~10^3 times lower than without prompt redeposition [3]

5. Discussion and conclusions

We have used EPED1+SOLPS predictions for pedestal height and the empirical dependence of the ELM parallel energy density on pedestal parameters to derive the expected parallel energy fluxes during ELMs in ITER. This has allowed the derivation of the boundaries of the operating space, where the uncontrolled ELMs will not cause unacceptable divertor erosion.

The analysis carried out by the application of the scaling in [4] together with the pedestal plasma pressure derived from EPED1+SOLPS scalings [5] indicates that ELM control for acceptable outer divertor erosion would not be required in ITER over a significant range of plasma currents and densities (see Fig. 1). The actual maximum plasma current values of the present estimates are typically somewhat higher than previous studies for q_{95} =3 assuming the same wetted area during ELMs than between ELMs [2] due to the new findings in [4] regarding the energy flux during ELMs and because in [2] it was assumed that the ELM energy flux at the inner divertor was a factor of 2 larger than at the outer one, which is now questionable on the basis of the new results in [4] showing a more symmetric distribution. For ITER plasmas the maximum plasma current considered operation such that the safety factor $q \geq 3$ ($q \sim B/I_p$) and thus, for half-field operation in H-mode where $I_p \leq 7.5$ MA no ELM control is required to achieve acceptable divertor erosion with optimistic assumptions, K=1. It is important to note that the corresponding ELM energy loss for these "acceptable" uncontrolled ELMs is large (typically ~ 10 MJ) and their frequency is low (typically f_{ELM} ~ 1-2 Hz) and W production by physical sputtering is significant which is expected to lead to L-H transitions. It is also important to note that operation at B_t = 5.3T restricts significantly the maximum current with "acceptable" uncontrolled ELMs due to the scaling of the pedestal pressure as $p_{ped} \sim I_p \times B_t$ in ITER plasmas and the decrease of the parallel area for energy flow as ~$1/B_t$. In addition limitations on the ELM size for H-mode operation also are found due to plasma contamination by tungsten, sputtered by ELMs, provided it could reach the core plasma (i.e. w/o prompt W re-deposition at the ELM).

For the simulations performed taking into account time-averaged W influxes, neoclassical screening of the W in the plasma pedestal is sufficient to keep H-mode operation even for the largest W influxes without prompt re-deposition both for P_{SOL} = 100 MW and P_{SOL}=50 MW

because the separatrix densities are sufficiently high to provide the efficient neoclassical screening of tungsten [14].

Full 1.5D modelling of plasma evolution with discrete ELMs and tungsten influx pulses shows that the limitations on the ELM size appear only if the pulses of tungsten sputtered by ELMs reach the core w/o prompt tungsten re-deposition. Without re-deposition ELMs of rather moderate size $\Delta W_{ELM} > 1.1$ MJ can produce W pulses that can increase core plasma radiation to a level sufficient to trigger back H-L transition and possible follow-up disruption in agreement with [3].

For ELMs smaller than this size another limitation can come from tungsten accumulation on long timescales. In this case the dominant transport process during the ELM strongly affects tungsten accumulation especially because tungsten is screening by neoclassical transport in the ITER pedestal. For ELMs modelled with a convective model the additional tungsten coming to the core after an ELM is efficiently pushed out by the following ELM. Thus, the inter-ELM evolution does not play a major role similar to [3], [15]. For ELMs modelled with a diffusive model, the ELM flattens the tungsten profile producing deeper penetration of tungsten after each ELM. Thus, for diffusive ELMs tungsten accumulates in the plasma core when the tungsten recovery time, t_W, is large, $f_{ELM} \times t_W = \alpha P_{sol}\, t_W / \Delta W_{ELM} \geq 1$. Our modelling with α=0.2 predicts no tungsten accumulation in the whole range of the ITER pellet pacing frequencies, $f_{ELM} = f_{pel} \leq 32$ Hz, while for P_{sol}=100 MW, f_{pel} = 32 Hz (ΔW_{ELM}=0.6 MJ) the conditions are marginal. For larger $\alpha = 0.4$, ΔW_{ELM}=1 MJ, f_{ELM}=40 Hz (α=0.4), the accumulation factor increases by a factor of ~ 2.5, and tungsten gradual accumulation will cause the reduction of $P_{sol}/P_{LH} \rightarrow 1$ and following transition to the L-mode, which is in agreement with ELM simulations in [15]. The choice of the proper model for particle expulsion during ELMs in ITER requires experimental studies in an ITER-like pedestal plasma. In most present experiments the pedestal impurity profile is peaked (i.e. inward neoclassical convection dominates), for which diffusive or convective model produce more or less the same result unlike in ITER. To have a more accurate assessment of the evaluation for ITER direct ASTRA–SOLPS coupling is required, which could be the subject of future work for further investigations.

Disclaimer: The views and opinions expressed herein do not necessarily reflect those of the ITER Organization

Acknowledgements

We are thankful to Dr. R. Pitts and Dr. A.S. Kukushkin for useful consultations, and to Dr. D.J. Campbell for support of our studies.

References

[1] A.R. Polevoi, et al., Nucl. Fusion, **56** (2016) (to be published)
[2] A. Loarte, et.al, Nucl. Fusion, **54** (2014) 033007
[3] R. Dux, et. al, "Influence of a Tungsten Divertor on the Performance of ITER H-Mode Plasmas", TH/P3-29, 25th IAEA Fusion Energy Conference, 13–18 October, 2014, Saint Petersburg, Russian Federation.
[4] T. Eich, et al, Proc. 22nd International Conference on Plasma Surface Interactions in Controlled Fusion Devices (PSI), 2016, Rome, Italy.
[5] A.R. Polevoi et. al, Nucl. Fusion, **55** (2015) 063019
[6] T. Eich et al. , J. Nucl. Mater., **415** (2011) S856–S859
[7] A. Hermann, Plasma Phys. Contr. Fusion **44** (2002) 883
[8] A. Loarte et al, Plasma Phys. Control. Fusion **44** (2002) 1815
[9] A.R. Polevoi and M. Shimada, Plasma Phys. Control. Fusion **43** (2001) 1525
[10] H.D. Pacher, et al, J. Nucl. Mater. **463** (2015) 591–595
[11] G.V. Pereverzev, et al, "ASTRA Automated System for TRansport Analysis", IPP-Report IPP 5/98 (2002).
[12] V.M. Leonov, V.E. Zhogolev, Plasma Phys. Control. Fusion, **47** (2005) 903
[13] Y.R. Martin, et al, Journal of Physics: Conference Series **123** (2008) 012033
[14] R. Dux, et al, Plasma Phys. Control. Fusion, **56** (2014) 124003
[15] D.P. Coster, et al, J. Nucl. Mater **463** (2015) 620